symmetry

MDPI

Article

Does the Presence of a Bond Path Really Mean Interatomic Stabilization? The Case of the Ng@Superphane (Ng = He, Ne, Ar, and Kr) Endohedral Complexes

Mirosław Jabłoński

Faculty of Chemistry, Nicolaus Copernicus University in Toruń, Gagarina 7, 87-100 Toruń, Poland; teojab@chem.umk.pl; Tel.: +48-056-611-4695

Abstract: Using a fairly structurally flexible and, therefore, very suitable for this type of research, superphane molecule, we demonstrate that the inclusion of a noble gas atom (Ng = He, Ne, Ar, and Kr) inside it and, thus, the formation of the Ng@superphane endohedral complex, leads to its 'swelling'. Positive values of both the binding and strain energies prove that encapsulation and in turn 'swelling' of the superphane molecule is energetically unfavorable and that the Ng···C interactions in the interior of the cage are destabilizing, i.e., repulsive. Additionally, *negative* Mayer Bond Orders indicate the *antibonding* nature of Ng···C contacts. This result in combination with the observed Ng···C bond paths shows that the presence of a bond path in the molecular graph does not necessarily prove interatomic stabilization. It is shown that the obtained conclusions do not depend on the computational methodology, i.e., the method and the basis set used. However, on the contrary, the number of bond paths may depend on the methodology. This is yet another disadvantageous finding that does not favor the treatment of bond paths on molecular graphs as indicators of chemical bonds. The Kr@superphane endohedral complex features one of the longest C–C bonds ever reported (1.753 Å).

Keywords: superphane; noble gas atom; endohedral complex; encapsulated; steric crowding; repulsion; destabilization; QTAIM; bond path; Mayer Bond Order

Citation: Jabłoński, M. Does the Presence of a Bond Path Really Mean Interatomic Stabilization? The Case of the Ng@Superphane (Ng = He, Ne, Ar, and Kr) Endohedral Complexes. *Symmetry* **2021**, *13*, 2241. https://doi.org/10.3390/sym13122241

Academic Editor: Steven Robert Kirk

Received: 25 October 2021
Accepted: 15 November 2021
Published: 24 November 2021

1. Introduction

One of the extremely useful methods in the study of various types of intra- and intermolecular interactions is Quantum Theory of Atoms in Molecules (QTAIM) by Bader [1–3]. One of the statements of this theory is particularly important because it undoubtedly had a huge impact on the development of knowledge regarding the theory of chemical bonding and on when chemists are to find such a bond between any pair of atoms. Namely, according to QTAIM (now sometimes called the orthodox QTAIM) we are to learn that, for any pair of atoms, the sufficient and necessary condition to say that they are bonded to one another is the simultaneous presence on a molecular graph (i.e., a network of bond paths) of a bond path (BP) linking their nuclei and a corresponding bond critical point (BCP) [1,4].

Indeed, this statement has become so ingrained in the minds of many scientists that they take the presence of a bond path (and a bond critical point) as the only evidence of a chemical bond between any pair of atoms. Worse still, this often happens even when many parameters, such as geometric parameters, indicate that something is wrong with the recalled statement. On the other hand, however, it is a fact that, in the case of many molecules (however, rather relatively simple and small), the molecular graph follows the structural formula [5], which justifies the applicability of this statement.

Cioslowski was the first to suggest that the presence of BP and the accompanying BCP is not necessarily associated with stabilizing interaction and that both these topological features could also be associated with a repulsive instead of attractive interaction [6–9]. As he demonstrated, such BPs would especially be generated in sterically crowded systems.

For this reason, although it does not exclude many other systems, the so-called endohedral complexes, i.e., complexes that create a relatively small space gap in which an atom, an ion, or a small molecule is trapped, seem to be particularly important.

Indeed, Haaland et al. [10,11] have investigated the nature of the 'repulsive bond paths' in He@adamantane, while Merino et al. studied the effect of symmetry on the bond paths in He@cubane, He@dodecahedrane, He_2@dodecahedrane, and Ng@C_{60} (Ng = He, Ne, Ar, and Kr) [12,13]. In the former two articles [10,11] it has been shown that the interaction between the encapsulated helium atom and the adamantane cage is actually destabilizing despite the presence of bond paths between the helium atom and the cage carbon atoms.

Merino et al. [13] demonstrated that the interaction between He_2 and the dodecahedrane cage is repulsive. Moreover, it was shown [12] that the presence of multiple BPs may result from the high symmetry of a system and does not necessarily mean a stabilizing effect, therefore, making the one-to-one analogy between BP and a chemical bond is risky [12].

It is important to mention here that BPs have been found in many unexpected (counterintuitive) cases. These cases most often correspond to the presence of BP between two highly electronegative atoms [6,9,14–30], especially those with large radii [16,28,29]. Representative examples are the O···O BPs in carbon dioxide dimer [14,15,28,29], $C(NO_2)_3^-$ ion [6,18,30], open conformers of enol forms of some cis-β-diketones [20], S···S BPs in, e.g., $(SCO)_2$ or $(CS_2)_2$ [29], Cl···O BP in 3-halogenopropenal [21–23], and F···F BPs in perhalogenated cyclohexanes, dodecahedranes, fulleranes [9], protonated perfluorodiether [17] and various difluorinated aromatic compounds (e.g., 1,8-difluoronaphtalene) [19].

Even earlier bond paths between two chlorine atoms were found in solid chlorine [14]. An equally important group are BPs between hydrogen atoms that are in close proximity to each other [31–35], such as the *ortho*-hydrogens in flat biphenyl [7,8,31–33] or the internal hydrogen atoms in kekulene [6,8]. Such H···H BPs have also been found in many other hydrocarbons [31], e.g., some planar benzenoids possessing phenanthrene moiety [8], styrene, Z-2-butene or 2,3-dimethyl-2-butene [35] More important examples of counterintuitive BPs are mentioned in the references [28–30].

As already mentioned, endohedral complexes are particularly interesting systems containing some controversial 'repulsive bond paths'. Thus far, the enclosing molecules studied have been adamantane ($C_{10}H_{16}$) [10,11], cubane (C_8H_8), dodecahedrane ($C_{20}H_{20}$), and C_{60} fullerene [12,13]. In the context of the research on the energetical stability of endohedral complexes, tetrahedrane (C_4H_4), bicyclo[2.2.2]-octane (C_8H_{14}), truncated tetrahedrane ($C_{12}H_{12}$), and $C_{16}H_{16}$ have also been analyzed [36]. Of course, the fundamental C_{60} fullerene has also been the subject of such research [37].

However, in the case of the vast majority of these molecules, the susceptibility to structural changes caused by the encapsulation of some entities inside their interiors is very limited, and therefore these molecules are regarded as rather very rigid systems. Consequently, the observation of changes in geometric parameters caused by placing an atom, an ion or a small molecule inside them is quite limited. This article uses a superphane (i.e., [2.2.2.2.2.2]-(1,2,3,4,5,6)cyclophane) molecule [38,39] (Figure 1) that belongs to a wider group of cyclophanes [40].

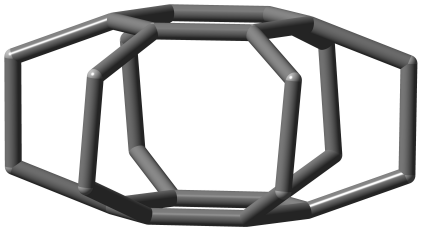

Figure 1. Superphane structure, omitting all hydrogen atoms.

As shown in Figure 1, superphane is a system of two parallel placed benzene rings connected with each other by six ethylene bridges (spacers). These ethylene bridges are structurally flexible enough that the presence of the host in the interior of the superphane cage is manifested in significant changes in certain bond lengths and angles, much greater than in all previously studied systems, e.g., adamantane, cubane, dodecahedrane, or the fullerene C_{60}. For this reason, Ng@superphane is a very suitable endohedral complex to study the effect of an encapsulated atom on a caging molecule. In particular, the purpose of this article is to answer the question of whether the Ng$\cdots$superphane interaction is stabilizing or destabilizing, and whether a bond path really means, as many still believe, the presence of a stabilizing interatomic interaction.

2. Methodology

The research systems used are superphane and its four endohedral complexes E@superphane, in which the He, Ne, Ar, or Kr atom is placed inside the superphane cage. In the first stage of the research, the influence of the level of theory (i.e., the method and the basis set) on the stability of the obtained results was examined. For this purpose, geometry optimizations of the considered systems were carried out using seven methods (HF [41], B3LYP [42,43], B3LYP-D3 [42–44], M06 [45], M06-HF [46], M06-2X [45], and ωB97X-D [47]) and three basis sets (6-31G, 6-31G(d), and 6-311G) for each of them, but ωB97X-D, for which nine basis sets [48,49] were used: 6-31G, 6-31G(d), 6-311G, 6-311G(d), 6-311G(d,p), 6-311+G(d), 6-311+G(d,p), 6-311++G(d,p), and 6-311++G(2d,p).

After geometry optimizations, analyses of the vibration frequencies were performed. All the structures obtained correspond to the true minima on the potential energy hypersurfaces. These calculations were made with the Gaussian 16 program [50]. Graphical representation of the molecules and the total energy curve were obtained with the GaussView 6 program [51], while molecular graphs were obtained with the AIMAll program [52].

The binding energy (E_b) between the encapsulated noble gas atom (Ng = He, Ne, Ar, Kr) and a superphane molecule was obtained as the difference between the total energies of the Ng@superphane endohedral complex, superphane, and the atom Ng:

$$E_b = E(\text{Ng@superphane}) - E(\text{superphane}) - E(\text{Ng}) \quad (1)$$

The same formula [53] was used, e.g., by Moran et al. [36] in their article on the viability of small endohedral complexes, although these authors used the name of the inclusion energy. Importantly, it should be noted that the binding (inclusion) energy defined in this way means stabilization of the Ng atom when this energy is negative and destabilization (resulting from internal repulsion) when this energy is positive. The strain (distortion) energy (E_{strain}) of the superphane, on the other hand, was simply calculated as the difference between the total energies of the superphane with its complex geometry and its equilibrium geometry, i.e., obtained after full optimization:

$$E_{strain} = E(\text{superphane}^{\star}) - E(\text{superphane}) > 0 \quad (2)$$

Clearly, the strain energy is positive, which results from the energetic disadvantage of structural changes.

The A–B bond order [54] was determined in two ways; using the very popular but somewhat outdated Wiberg Bond Index (WBI) [55]:

$$\text{WBI}_{AB} = \sum_{\alpha \in A} \sum_{\beta \in B} \boldsymbol{P}^2_{\alpha\beta} \quad (3)$$

and the newer Mayer Bond Order (MBO) [56–59]:

$$\text{MBO}_{AB} = \sum_{\alpha \in A} \sum_{\beta \in B} (\mathbf{PS})_{\alpha\beta} (\mathbf{PS})_{\beta\alpha} \quad (4)$$

which can be investigated as an extension of WBI. In these formulas, **P** and **S** are the density and the atomic orbital overlap matrices, respectively. Note that, while WBI must be positive by definition, MBO can also be negative. As will be shown, this rather very rare and unusual possibility will prove to be significant because it indicates an antibonding effect between atoms A and B.

3. Results and Discussion

3.1. Methodological Stability of the Results

One of the aims of the article was to show that the main conclusions do not depend on the level of theory, i.e., on the adopted computational protocol. Therefore, at the beginning, the results proving the methodological stability of the conclusions obtained are presented. In order to significantly reduce the amount of numerical data, this presentation is limited to the binding energy (E_b) and the distance C···C between the benzene rings of superphane ($d_{\pi\cdots\pi}$).

The former of these parameters is crucial in this article, while the later experiences the greatest changes upon both the change of method or basis set and the Ng atom itself. The values of E_b and $d_{\pi\cdots\pi}$ obtained with the use of seven methods and three basis sets are presented in Tables 1 and 2, respectively.

The results presented in both tables, i.e., Tables 1 and 2, show that the obtained values only slightly depend on the basis set used in the calculations (what is more, the basis sets used here are rather small) and the methods, although in the latter case it is clearly visible that the values obtained using the HF method differ from the results obtained by the DFT [60,61] method. However, this was to be expected, as the HF method differs from the DFT method, for example, in that it does not take into account the interelectron correlation effects [41,48]. The most important issue, however, is that the individual noble gas atoms form well-separated ranges of values, so that any (rather small) differences resulting from different methodologies are much smaller and, therefore, will not qualitatively affect the obtained conclusions.

To check the dependence of the results on the basis set used in the calculations even more thoroughly, more basis sets were used–larger and therefore more reliable. This check was performed only for ωB97X-D [47], which is one of the best functionals for general use [62]. The obtained values of E_b and $d_{\pi\cdots\pi}$ are presented in Table 3.

The obtained ranges of values show that the sensitivity of E_b and $d_{\pi\cdots\pi}$ to the basis set used increases with increasing size of the noble gas atom, i.e., in the order He→Ne→Ar→Kr. These ranges, however, are negligible in relation to the average value, as indicated by the negligible percentages $\%_{av.}$, especially for $d_{\pi\cdots\pi}$, i.e., the distance C···C.

Table 1. The binding energy (in kcal/mol) of the encapsulated Ng atom with a superphane molecule.

Ng	Basis Set	HF	B3LYP	B3LYP-D3	M06	M06-HF	M06-2X	ωB97X-D
He	6-31G	94.0	81.5	79.3	79.9	80.0	77.7	82.5
	6-31G(d)	93.9	82.2	79.9	80.8	80.8	78.1	83.1
	6-311G	94.0	81.8	79.6	80.1	80.1	77.4	82.8
Ne	6-31G	230.2	192.8	189.3	193.5	193.5	190.4	199.4
	6-31G(d)	225.4	188.6	185.1	189.8	189.8	186.7	195.0
	6-311G	229.8	196.1	192.6	195.6	195.6	192.5	201.0
Ar	6-31G	527.7	454.0	451.8	445.5	445.5	448.1	459.7
	6-31G(d)	510.4	438.2	436.3	431.0	431.0	432.6	443.1
	6-311G	523.1	450,5	448.4	443.7	443.7	444.3	456.6
Kr	6-31G	638.7	545.6	544.8	534.1	534.1	541.8	551.4
	6-31G(d)	624.8	out [a]	out [a]	out [a]	out [a]	530.0	538.7
	6-311G	654.4	561.7	561.1	552.2	552.1	559.4	569.5

[a] The full geometry optimization of Kr@superphane leads to the ejection of Kr outside the superphane cage. See further comment.

Table 2. The distance C$\cdots$C (in Å) between the benzene rings of superphane ($d_{\pi\cdots\pi}$).

Ng	Basis Set	HF	B3LYP	B3LYP-D3	M06	M06-HF	M06-2X	ωB97X-D
	6-31G	2.656	2.666	2.669	2.647	2.648	2.659	2.657
	6-31G(d)	2.663	2.662	2.666	2.648	2.648	2.658	2.655
	6-311G	2.659	2.667	2.670	2.645	2.646	2.659	2.657
	6-31G	2.814	2.834	2.838	2.819	2.819	2.821	2.820
He	6-31G(d)	2.826	2.836	2.841	2.823	2.823	2.827	2.825
	6-311G	2.818	2.836	2.840	2.816	2.816	2.823	2.820
	6-31G	3.114	3.140	3.144	3.128	3.128	3.134	3.120
Ne	6-31G(d)	3.123	3.139	3.148	3.127	3.128	3.137	3.123
	6-311G	3.118	3.142	3.146	3.129	3.130	3.136	3.122
	6-31G	3.594	3.621	3.627	3.597	3.597	3.611	3.596
Ar	6-31G(d)	3.569	3.591	3.595	3.567	3.568	3.590	3.571
	6-311G	3.591	3.620	3.625	3.594	3.594	3.612	3.593
	6-31G	3.719	3.766	3.765	3.735	3.735	3.751	3.734
Kr	6-31G(d)	3.690	out [a]	out [a]	out [a]	out [a]	3.724	3.700
	6-311G	3.720	3.766	3.765	3.733	3.732	3.752	3.731

[a] The full geometry optimization of Kr@superphane leads to the ejection of Kr outside the superphane cage. See further comment.

Table 3. The binding energy (in kcal/mol) of the encapsulated Ng atom within a superphane molecule and the distance C$\cdots$C (in Å) between the benzene rings of superphane.

Basis Set	$E_{\mathbf{int}}$				$d_{\pi\cdots\pi}$				
	He	Ne	Ar	Kr	∅	He	Ne	Ar	Kr
6-31G	82.5	199.4	459.7	551.4	2.657	2.820	3.120	3.596	3.734
6-31G(d)	83.1	195.0	443.1	538.7	2.655	2.825	3.123	3.571	3.700
6-311G	82.8	201.0	456.6	569.5	2.657	2.820	3.122	3.593	3.731
6-311G(d)	83.4	199.0	440.4	553.7	2.656	2.826	3.132	3.574	3.706
6-311G(d,p)	80.8	199.4	440.8	553.9	2.654	2.818	3.130	3.574	3.706
6-311+G(d)	83.0	201.7	437.9	551.2	2.655	2.826	3.131	3.568	3.703
6-311+G(d,p)	80.6	202.0	438.4	551.5	2.653	2.818	3.130	3.569	3.703
6-311++G(d,p)	80.7	202.1	438.4	551.5	2.654	2.819	3.130	3.568	3.703
6-311++G(2d,p)	81.3	201.4	436.5	551.6	2.650	2.817	3.126	3.562	3.698
Range	2.8	7.1	23.2	30.8	0.007	0.009	0.012	0.034	0.036
$\%_{\mathrm{av.}}$	3.4	3.5	5.2	5.6	0.3	0.3	0.4	1.0	1.0

It is worth emphasizing that both in view of the generally relatively small ranges of changes in the analyzed values and, importantly, the separation of value ranges due to the type of the Ng atom, the conclusions discussed further could also be obtained by means of the smallest (and least reliable) of the basis sets used here, 6-31G. Nevertheless, following the generally accepted principle to use the largest possible basis set, further analysis will be based on the results obtained by means of the largest 6-311++G(2d,p) basis set (and the ωB97X-D exchange-correlation functional), i.e., at the ωB97X-D/6-311++G(2d,p) level of theory.

3.2. Is the Ng$\cdots$Superphane Interaction in the Ng@Superphane Complex Stabilizing?

3.2.1. Energy and Structural Arguments

It is understandable that encapsulating an atom into the interior of the superphane molecule will affect its physicochemical properties and its structure. It should be expected that this influence will be more pronounced the bulkier the encapsulated atom is. The relatively high flexibility of the superphane molecule structure allows for an elegant visualization of these changes. The values (ωB97X-D/6-311++G(2d,p)) of the binding energy, the strain energy, and the selected geometric parameters for the superphane and

Ng@superphane complexes are presented in Table 4. For a better visualization of changes, the considered distances and energies are also shown in Figure 2.

Table 4. The binding and strain energies (in kcal/mol) and the selected geometric parameters (in Å or degrees) for the superphane molecule (∅) and Ng@superphane (Ng = He, Ne, Ar, and Kr) complexes.

Ng	E_b	E_{strain}	$E^{\%}_{strain}$	$d_{\pi\cdots\pi}$	d^{spacer}_{C-C}	d^{ring}_{C-C}	α_{CCC}	θ_{CCCC}
∅	n/a	0.0	n/a	2.650	1.591	1.404	110.3	6.3
He	81.3	8.7	10.7	2.817	1.601	1.415	113.3	7.7
Ne	201.4	59.5	29.5	3.126	1.630	1.428	118.8	9.3
Ar	436.5	186.8	42.8	3.562	1.707	1.444	126.0	7.9
Kr	551.6	241.6	43.8	3.698	1.753	1.429 [a]	127.8	2.0 [a]
						1.482 [a]		4.0 [a]

[a] A pair of significantly different values has been found that alternates.

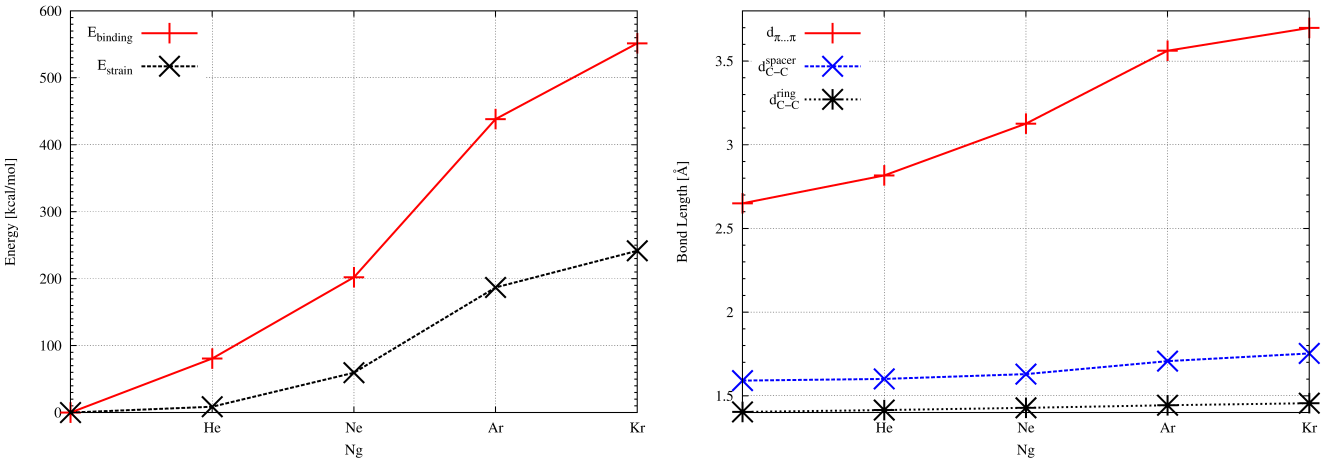

Figure 2. Dependence of the distance $d_{\pi\cdots\pi}$, the length of the bonds d^{spacer}_{C-C} and d^{ring}_{C-C} (**left**) and the binding and strain energy (**right**) on the noble gas atom (Ng = He, Ne, Ar, and Kr) in the endohedral Ng@superphane complex.

What is most important is that the binding energies are clearly positive, and therefore, according to the definition given by Equation (1), they indicate the fact that the Ng$\cdots$superphane interactions inside the cage are *destabilizing*. It should be noted that positive binding energies, indicating an internal *repulsive* effect, were obtained for the vast majority of endohedral complexes [10–12,36,37]. This result reflects the fact that both entities, i.e., Ng and superphane, prefer not to form an endohedral complex with each other, but rather to be separated from each other. This conclusion is consistent with the statement of Moran et al. that "... exohedral coordination is preferred to endohedral complexes without exceptions." [36].

As expected, the destabilization effect of the endohedral Ng@superphane complex increases monotonically as the size of the noble gas atom increases (Table 4 and Figure 2). The binding energy is as high as 551.6 kcal/mol for the Kr atom. It is also true that, in general, the binding energy depends on the size of the cage, e.g., for the smaller adamantane and even yet smaller cubane the binding energy with the encapsulated helium atom is as high as 154.7 kcal/mol (B3LYP/6-311++G(2d,2p)) [10,11] and 322.4 kcal/mol (B3LYP/6-311++G(d,p)) [12], respectively, while for He@superphane it is only 81.3 kcal/mol (Table 4).

The encapsulated noble gas atom has a significant impact on the structure of the Ng@superphane complex. It is especially visible during the analysis of the distance between benzene rings, i.e., $d_{\pi\cdots\pi}$. This distance in a superphane is 2.650 Å. Encapsulation of a helium atom inside it leads to an increase in this distance to 2.817 Å, i.e., by 0.167 Å, which gives ca. 6% of the initial distance. The exchange of He to Ne leads to a further increase to 3.126 Å, i.e., a further 0.309 Å, or 11%, an increase of 18% over the superphane value. The effect of the exchange of Ne on Ar is very significant. The distance $\pi\cdots\pi$

increases by a further 0.436 Å (to 3.562 Å), or 14%, which is more than a third (34%) of the value in the superphane molecule. Replacing the Ar atom with the Kr atom, however, does not cause such a significant change (0.136 Å, i.e., ca. 4%). Nevertheless, in relation to superphane, the distance $\pi \cdots \pi$ increases by 1.048 Å, which is 40%. This result best confirms the considerable flexibility of the superphane cavity, which makes the superphane molecule a convenient species for research on the effect of encapsulation.

It should be remembered that both benzene rings of the superphane molecule are bound together by six ethylene bridges (see Figure 1). It should be expected that the distancing of the benzene rings from each other, forced by encapsulation of the noble gas atom, has an unfavorable effect on the structure of these bridges. First of all, as can be seen from Table 4 (and Figure 2), the C-C bond undergoes a significant and monotonic elongation, from 1.591 Å in superphane to 1.753 Å in Kr@superphane, i.e., by 10%. It is worth mentioning that it is one of the longest C–C bonds ever reported [63–65], not including record breaking carboranes [66–68] and especially tetracyanoethylene [69] and tetracyanopyrazinide [70] dimer dianions.

Encapsulation changes the value of the C-C-C angle in the bridge (α_{CCC}) from the favorable characteristic for the tetrahedron (about 109.5°) to the unfavorable one, amounting to as many as 128° in the complex containing the largest Kr atom. It is also worth emphasizing that encapsulation with a larger and larger Ng atom leads to the elongation of C-C bonds in the benzene rings, from 1.406 Å in superphane to 1.456 Å (on average) in Kr@superphane. An interesting fact is that the full geometry optimization of the Kr@superphane complex leads to a clear distinction between C-C bonds in benzene rings, so that they have two different lengths (1.429 and 1.482 Å) and alternate. This change shows that benzene rings are no longer aromatic.

It is worth noting that, as indicated by the values of the dihedral angle θ_{CCCC} shown in the last column of Table 4, the ethylene bridges are slightly twisted and the $C_{ring}C_{Et}C_{Et}C_{ring}$ carbons are not in one plane. Such a defect is most likely aimed at minimizing the unfavorable angular stresses in the ethylene connectors. This angle in the case of superphane amounts to ca. 6° and increases slightly (by ca. 1–3°) in complexes with He, Ne or Ar. On the other hand, in the case of the Kr@superphane complex, significantly lower values (2.0° and 4.0°) and their alternation (similar to the C-C ring bond) have been obtained.

It is clear that the structural changes caused by encapsulation are adverse to the host superphane molecule. Apart from the already discussed structural changes, a strong energetic destabilization of the superphane should be expected. This destabilization can be easily described by the strain energy defined by Equation (2). As can be seen from Table 4 and Figure 2, this energy actually increases rapidly from 8.7 kcal/mol in He@superphane to as much as 241.6 kcal/mol in Kr@superphane, which is ca. 11% and as much as 44% of the binding energy. It is clear that the strain energy should depend to a large extent on the volume of the cavity inside the encapsulating molecule. For example, this energy is as high as 15.3 kcal/mol for the He@adamantane complex [10,11].

The values of the structural parameters presented in Table 4 are sufficient to conclude that the superphane molecule 'swells' as soon as an atom of noble gas is introduced into it. This effect is greater the larger this atom is. Of course, this effect is energetically unfavorable for the superphane molecule, as evidenced by the rapid increase in the strain energy. It is possible that increasing the atom's size to Xe and Rn will disrupt the endohedral complex while releasing the encapsulated noble gas atom. Of course, it is to be expected that this process will be associated with the release of energy.

This will be the subject of future research. Nevertheless, an additional result clearly indicating an unfavorable energetics of the Kr@superphane endohedral complex is the result of its full optimization which has been obtained utilizing the 6-31G(d) basis set together with some exchange-correlation functionals (see Tables 1 and 2). Although this result may be due only to a fairly small basis set 6-31G(d) (although it did not occur in the case of the even smaller 6-31G and using the Hartree–Fock method or either the M06-2X or

ωB97X-D exchange-correction functional), it is worth discussing, which is presented in the next subsection.

3.2.2. About How Krypton Escapes from the Cage

In the footnotes to Tables 1 and 2, it has already been mentioned that the full geometry optimization of the Kr@superphane endohedral complex leads in some cases to the spontaneous expulsion of the Kr atom from the superphane cage, which of course leads to a decrease in the total energy of the Kr–superphane system. This interesting result has been obtained in the case of geometry optimizations utilizing B3LYP, B3LYP-D3, M06, or M06-HF exchange-correlation functionals, but only together with the basis set 6-31G(d).

However, this result has not occurred in the case of the M06-2X and ωB97X-D functionals or the methodologically simpler Hartree–Fock method. Moreover, all of these methods have not given this result as long as either the 6-31G or the 6-311G basis set was used (see Tables 1 and 2). Therefore, on the one hand, this result could be considered as an artifact (which, however, has happened), but on the other hand, it is possible that some other basis sets and some other functionals (and there are hundreds of both [49,62]) would lead to this the same result, i.e., to a spontaneous ejection of the trapped krypton atom out of the superphane cage.

Of course, although the search for other method/basis set combinations may be a student project (albeit rather arduous), it was not the main goal of the research described here. Nevertheless, it is worth taking a look at the total energy change that occurs during the optimization procedure. The B3LYP-D3/6-31G(d) case is shown in Figure 3. It represents the other three cases mentioned earlier.

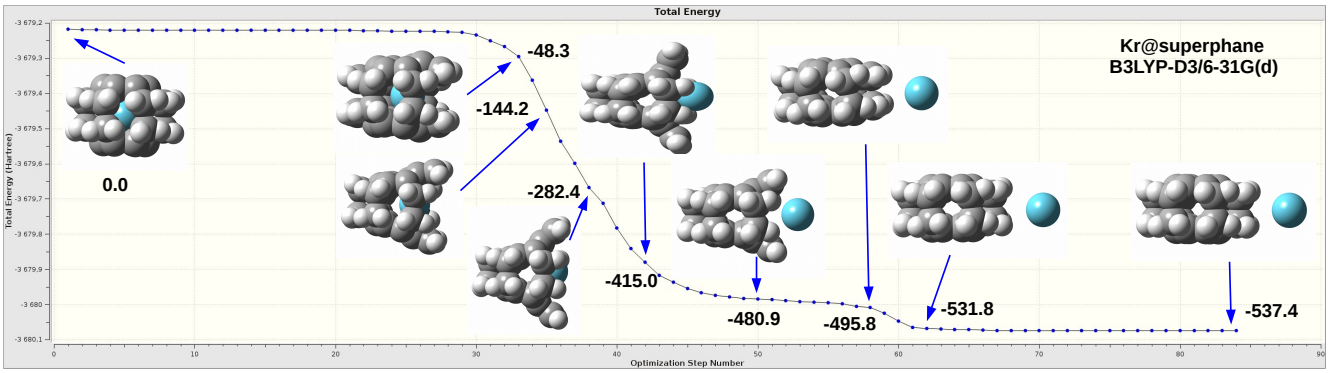

Figure 3. Changes in the total energy of the Kr@superphane complex during the optimization of its geometry at the B3LYP-D3/6-31G(d) level of theory. Selected structures and their energies (in kcal/mol) in relation to the initial structure are also shown.

Figure 3 clearly shows that when optimizing the geometry of the initially endohedral Kr@superphane complex, spontaneous (i.e., without any energy barrier) expulsion of the encapsulated krypton atom out of the superphane cage with simultaneous formation of the exohedral superphane$\cdots$Kr complex takes place. It is worth noting that, after this process, the superphane molecule is closed again and significantly flattened. The entire process of releasing the krypton atom is strongly exoenergetic, as much as 540 kcal/mol is released. It is also worth noting that even a slight opening of the cage of 'swollen' superphane is very energetically beneficial. The moment when the initially trapped atom Kr is in the carbon window is already an energy gain of about 150–250 kcal/mol.

In our opinion, this process is a powerful illustration of the intra-cage repulsion of the Kr$\cdots$superphane type (or more generally Ng@host). The fact that this process has not been observed at many other levels of theory is not at all evidence of the attractive interaction of the Ng$\cdots$host type, but simply because, at a given level of theory, disrupting the host cage is too energetically expensive. As is well known, the purpose of geometry optimization is to find the equilibrium structure, i.e., the most favorable energetically, which is related to the minimization of the total energy during its course.

For this reason alone, in most cases, we do not observe the removal of the encapsulated entity outside the host's cage, and this is by no means a symptom of a beneficial attractive interaction inside the cage. In the case of the previously described encapsulating hydrocarbons [36], such as, for example, adamantane [10,11], cubane [12,13], dodecahedrane [12,13], or fullerenes (e.g., the most famous C_{60} [12,13,37]) CC bonds are too strong to break, and therefore the encapsulated entity cannot spontaneously escape beyond the host's cage while optimizing the geometry of the E@host complex. It seems that superphane is also unique in this respect and is therefore suitable for research on the influence of an encapsulated entity on the properties of a host molecule.

3.2.3. On Whether a Bond Path Really Is Evidence of a Stabilizing Interatomic Interaction

As already mentioned in the Introduction, Cioslowski suggested for the first time that in some cases, especially in highly steric congested systems, a bond path may be associated with a repulsive rather than an attractive interatomic interaction [6–9]. Since then, there has been a wealth of literature on the subject [10–13,22–35]. Merino et al. [12] pointed out that a large number of bond paths terminating at an atom may be the result of a high symmetry of a system. For example, in the case of the He@cubane complex, they have found eight He$\cdots$C bond paths, while Ar@C_{60} experiences as many as 60 Ar$\cdots$C bond paths [12].

In the case of the Ng@superphane (Ng = He, Ne, Ar) complexes, in the vast majority of cases (depending on the Ng atom itself as well as the adopted level of theory), we have obtained 12 bond paths between the Ng atom and all the carbon atoms forming the benzene rings, but the picture becomes much more complicated in the case of the Kr@superphane complex. In the context of the ongoing discussion, this fact deserves more attention. Only four molecular graphs obtained using basis sets 6-31G, 6-311+G(d), 6-311++G(d,p), and 6-311++G(2d,p) together with the ωB97X-D functional are presented in Figure 4.

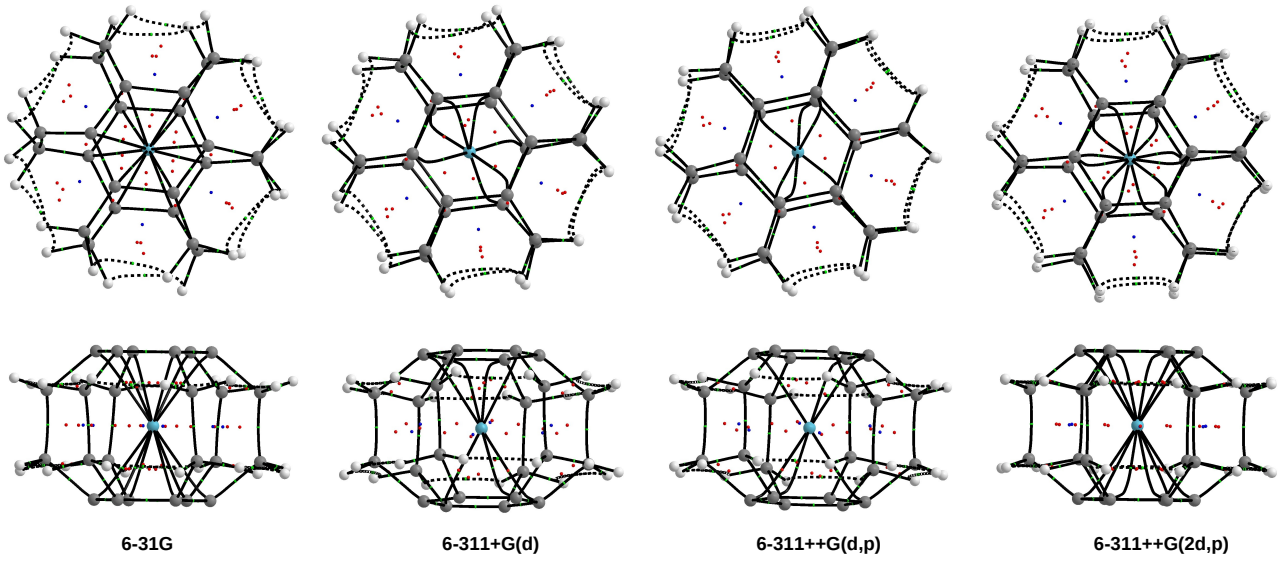

Figure 4. Molecular graphs of the Kr@superphane complex obtained with four different basis sets (6-31G, 6-311+G(d), 6-311++G(d,p), 6-311++G(2d,p)) and the ωB97X-D exchange-correction functional. Two shots are shown: top view (slightly tilted to avoid atomic overlapping and to facilitate counting of the bond paths to Kr atom) and side view.

Figure 4 shows that, depending on the basis set used to determine the molecular graph of Kr@superphane, 12 (6-31G and 6-311++G(2d,p)), 7 (6-311+G(d)) or only 6 (6-311++G(d,p)) Kr$\cdots$C bond paths have been obtained. Since the number of chemical bonds cannot be so easily varied, it is clear that a bond path cannot mean a chemical bond. It is also worth noting that although basis sets 6-31G and 6-311++G(2d,p) have led to the same number (12) of Kr$\cdots$C bond paths, these paths differ significantly from each other. Namely, they are straight (and on the vertical planes of the rings) in the former case,

whereas clearly curved in the latter. Also, the change of the number of bond paths when changing the basis set 6-311++G(d,p) to 6-311++G(2d,p), and thus only after doubling the number of d-type functions on C and Kr atoms, should be of concern; does the number of bonds Kr···C change?

Other examples of the dependence of a molecular graph on the level of theory have recently been shown [28–30,71]. Two such cases will be mentioned here. The first one concerns the O···O type bond paths in the fully optimized $C(NO_2)_3^-$ anion [30] (Figure 5). Data concerning the presence of the O···O bond paths are presented in Table 5.

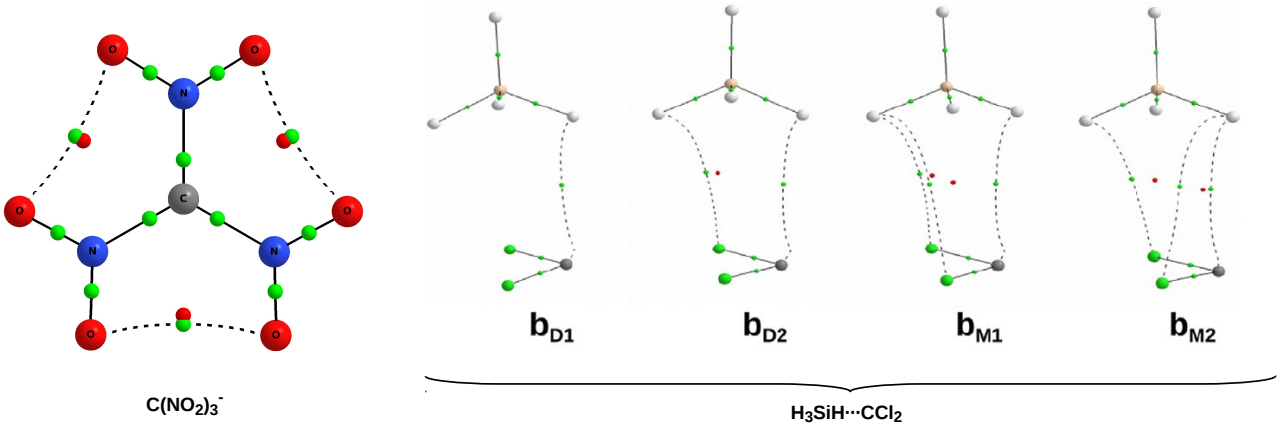

Figure 5. The case of the molecular graph of $C(NO_2)_3^-$, in which the O···O bond paths are present (**left**) and molecular graphs of the $H_3SiH\cdots CCl_2$ dimer obtained using different levels of theory (D = ωB97X-D, M = MP2, 1 = 6-311++G(2df,2pd), 2 = aug-cc-pVTZ (**right**).

Table 5. Dependence of the presence (YES) or absence (NO) of the O···O bond path in the fully optimized twisted form of $C(NO_2)_3^-$ [30].

Basis Set	HF	B3LYP	M06-2X	ωB97X-D	MP2
6-31G	YES	YES	YES	YES	NO
6-31G(d,p)	YES	YES	YES	YES	YES
6-311G(d,p)	YES	YES	YES	YES	YES
6-311++G(d,p)	YES	YES	YES	YES	NO
6-311++G(2df,2pd)	YES	NO	YES	NO	NO
cc-pVDZ	YES	YES	YES	YES	YES
cc-pVTZ	YES	NO	YES	NO	NO
cc-pVQZ	YES	NO	YES	NO	NO
aug-cc-pVDZ	YES	YES	YES	YES	YES
aug-cc-pVTZ	YES	NO	YES	NO	NO
aug-cc-pVQZ	YES	NO	YES	NO	n/c

Indeed, the results presented in Table 5 show that the presence of a given bond path (O···O in this case) in the molecular graph can be highly dependent on the methodology used. More specifically, within the set of considered basis sets, the presence of the O···O bond path is not dependent on the basis set when either the Hartree–Fock method or the M06-2X functional is used, while this dependence is manifested in the case of B3LYP, ωB97X-D and the second-order Møller–Plesset perturbation theory (MP2) [72].

In these cases, larger and better balanced basis sets (6-311++G(2df,2pd), cc-pVTZ, cc-pVQZ, aug-cc-pVTZ, aug-cc-pVQZ) did not give the O···O bond path, although it does not seem to be the rule, because the smallest basis set 6-31G in combination with MP2 also did not give such a bond path. This result also showed that a molecular graph obtained with a large and more reliable basis set can sometimes also be obtained with a much smaller and less reliable basis set [30]. The case of Kr@superphane molecular graphs shown in

Figure 4 also proves this very well. Namely, the smallest and generally unreliable basis set 6-31G reproduces (neglecting the clear differences in the curvature of the bond paths) the molecular graph obtained using the largest and most reliable 6-311++G(2d,p), whereas the slightly simpler form of the latter, i.e., 6-311++G(d,p), gives different number of bond paths. Therefore, the dependence of a molecular graph on the computational methodology makes the reliability of the molecular graph a somewhat problematic issue.

The second case is a bit more complex and concerns the presence of different types of bond paths on molecular graphs while using different methodologies. The molecular graphs obtained [71] with the four levels of theory for the $H_3SiH\cdots CCl_2$ dimer are shown in Figure 5. The use of the ωB97X-D/6-311++G(2df,2pd) level of theory ($\mathbf{b_{D1}}$) yielded only one intermolecular bond path, namely of the H$\cdots$C type. The use of the aug-cc-pVTZ basis set (i.e., the ωB97X-D/aug-cc-pVTZ level of theory; $\mathbf{b_{D2}}$) provided an additional H$\cdots$Cl bond path. In contrast, the MP2 method led to three bond paths for intermolecular interactions. Two of them are of the H$\cdots$Cl type, while one is of H$\cdots$C. However, both of these basis sets differentiate hydrogen atoms due to the number of such paths. Namely, in the case of the smaller 6-311++G(2df,2pd) basis set ($\mathbf{b_{M1}}$), one of the hydrogen atoms of SiH_4 is linked with two chlorine atoms of CCl_2. However, in the case of the larger aug-cc-pVTZ basis set ($\mathbf{b_{M2}}$), the same hydrogen atom creates a bond path to only one chlorine.

Returning to the main issue, however, whether a bond path must necessarily prove a stabilizing effect (especially in the case of endohedral complexes), it should be remembered that the encapsulation of the noble gas atom inside the superphane molecule has led to its high destabilization. As mentioned earlier, in the vast majority of cases of endohedral complexes, the trapped entity does not escape from the cage during the geometry optimization procedure just because the barrier associated with opening of the cage is too large to be overcome (nevertheless, such spontaneous ejection of the encapsulated entity is, indeed, possible as shown in the example of Kr@superphane in Figure 3).

The combination of the presence of counterintuitive Ng$\cdots$C bond paths with a simultaneous strong destabilization of the endohedral complex and therefore the urgent desire to eject the encapsulated atom out of the cage is, in our opinion, sufficient evidence to conclude that the presence of a bond path does *not* necessarily indicate interatomic stabilization (attraction).

3.2.4. Negative Mayer Bond Orders

The strength of a chemical bond is often described by the bond order. Still a popular variety of this property is the so-called Wiberg Bond Index (WBI) [55], which, however, is already somewhat outdated. Bridgeman et al. [59] have shown that the newer Mayer Bond Order (MBO) [56–58] is a very valuable parameter. Importantly, its definition (see Equation (4)) also allows for negative values. The calculated MBO values for the Ng$\cdots$C contact and for the C-C bond of the ethylene spacer and the benzene ring are shown in Table 6. Additionally, their WBI counterparts are also shown for comparison.

Table 6. Wiberg Bond Index (WBI) and Mayer Bond Order (MBO) for the Ng$\cdots$C contact and the C-C bonds (spacer and ring) in the superphane molecule (∅) and Ng@superphane (Ng = He, Ne, Ar, and Kr) complexes.

	WBI			MBO		
Ng	**Ng$\cdots$C**	**C-C$_{spacer}$**	**C-C$_{ring}$**	**Ng$\cdots$C**	**C-C$_{spacer}$**	**C-C$_{ring}$**
∅	–	0.96	1.37	–	0.98	1.40
He	0.007	0.97	1.37	−0.001	1.00	1.43
Ne	0.012	0.97	1.37	−0.065	1.01	1.58
Ar	0.016	0.95	1.38	−0.180	1.04	1.54
Kr	0.020	0.94	1.26 [a]	−0.902	1.15	1.57 [a]
			1.49 [a]			1.67 [a]

[a] A pair of significantly different values has been found that alternates.

As would be expected, the WBI value for the C-C spacer bond is close to 1 as it should be for a single bond. The WBI value for the C-C bond within the benzene ring is 1.37 and is slightly lower than the corresponding value for benzene (1.44). In the case of the Kr@superphane complex, a variation in value has been obtained which corresponds to a variation in length (see Table 4). More importantly, however, in the case of the Ng···C contacts, very small values, close to zero, have been obtained, which suggests negligibly weak Ng···C interactions.

However, it is instructive now to look at the Mayer Bond Orders (MBO). The corresponding values for the C-C spacer bond are again close to 1, and for the ring C-C slightly lower than or very similar to the benzene value (1.57). For Kr, two values have been obtained again. The most important result, however, is that the MBO values for the Ng···C contacts are negative! This result indicates the *anti*bonding nature of the interaction between the noble gas atom and the ring carbon atoms of the superphane molecule. The antibonding nature of this interaction increases with increasing size of the noble atom, i.e., He→Ne→Ar→Kr, and in the case of Kr it is significant (−0.902). It can be added that we have also obtained negative MBO values, e.g., for the He dimer with an interatomic distance of 2 Å (−0.003), or the $F^- \cdots F^-$ dimer (−0.035 for 3 Å and as much as −0.290 for 2 Å).

The obtained values of the bond order for C-C bonds slightly increase with the increase in the size of the Ng atom, while in the case of WBI these changes are negligible. This result may seem very astonishing, as a larger bond order should, according to Pauling's formula ($BO = e^{-(r-r_0)/b}$) [54], mean a shorter bond, but the C-C bonds actually become longer (the superphane 'swelling' effect) as the noble gas atom becomes larger (see Table 4). The Mayer Bond Order, however, depends on the charge delocalization [59] and the increase in value is most likely due to the strong charge transfer from the noble gas atom to the carbon atoms of the caging superphane molecule. As a result of this electron density transfer, the Ng atoms have partial positive charges.

3.3. Metastable Systems vs. Endohedral Complexes: Repulsion in a Chemical Bond?

The argument made by Krapp and Frenking [73] that the 1997 IUPAC definition of a chemical bond [74] does not require the interaction between the atoms that make up the molecule or aggregate to be attractive is not convincing in our opinion. Indeed, there are metastable molecules as exemplified by, e.g., He_2^{2+} with a lifetime of about 3 h [75–78], but in these cases there is no external factor that prevents or at least significantly hinders spontaneous dissociation into individual components. On the contrary, in the case of endohedral (inclusion) complexes, this is not the case.

Simply put, in the vast majority of such cases, the trapped atom cannot get out of the cage, as it would require too much energy. This does not mean, however, that this atom forms any chemical bond with the inner surface of this cage. What an encapsulated atom would prefer to do, whether to stay in or out of the cage, can easily be shown by some modification (especially widening) of the launch channel, as has been convincingly shown by Strenalyuk and Haaland [11]. For the appropriate combination of an encapsulating molecule and the encapsulated entity, spontaneous process of strong structural remodeling of the E@host complex [36] or even removal of the guest outside the host molecule with possible energetically advantageous exohedral complex formation [36] are also possible. The case of such a spontaneous removal of the initially encapsulated Kr atom from the interior of a superphane molecule, illustrated in Figure 3, shows it well. Therefore, we fully agree with the conclusion given by Strenalyuk and Haaland that "it is the attractive interactions that lead to the formation of an aggregation, while the repulsive interactions oppose it" [11]. However, the existence of 'repulsive bond paths' is a fact, so they cannot express the presence of a chemical bond.

4. Conclusions

Contrary to the orthodox QTAIM method, it has been shown that the presence of a bond path between a pair of atoms does not necessarily indicate stabilizing interaction between them. This conclusion essentially arises from two fundamental observations that obstruct QTAIM. First, as is known, counterintuitive bond paths are observed, e.g., in endohedral complexes, but in the vast majority of cases, the binding energy of the encapsulated entity (an atom, an ion, a small molecule) is positive, which proves the energetic disadvantage of the formation of such a complex. This leads to unfavorable structural changes in the host molecule.

The investigated encapsulating molecules studied so far (e.g., cubane, adamantane, dodecahedrane, fullerene C_{60}) are generally too rigid for unfavorable structural changes to be large and for the trapped entity to spontaneously escape out of the host's cage. However, this article uses a superphane molecule whose structural flexibility is very convenient for this type of research. Indeed, the changes in the geometrical parameters due to the inclusion of the noble gas atom inside the superphane molecule and thus the formation of the endohedral Ng@superphane complex are considerable.

In particular, significant elongations of the C–C bonds in the bridging ethylene groups that keep the benzene rings together have been observed. In fact, the longest C–C bond found in the Kr@superphane complex (1.753 Å) belongs to the longest C–C bonds reported so far, excluding carboranes and some dimer dianions. The most significant change, however, concerns the distance between the superphane benzene rings, which increases by up to 40%, from 2.650 Å in superphane to 3.698 Å in Kr@superphane. To use colloquial language, one can simply say that the superphane molecule 'swells' with the increase of the radius of the Ng atom, i.e., in the order He→Ne→Ar→Kr.

All the observed structural changes are energetically unfavorable, as evidenced by the *positive* and systematically increasing (in the order: He→Ne→Ar→Kr) values of the binding and strain energies. The highest values of both these energies have been obtained for the Kr@superphane complex, which amount to 551.6 and 241.6 kcal/mol, respectively. The methodological stability of the obtained conclusions was also checked. It was shown that the method and the basis set used in the calculations have no influence on the observed trends and the conclusions obtained.

Another issue that does not favor treating a bond path as a chemical bond is the fact that a molecular graph may depend on the adopted computational methodology. It is shown that the number of Kr···C bond paths in the Kr@superphane complex depends on the basis set and is 6, 7 or 12. What should be worrying, a small change in the basis set from 6-311++G(d,p) to 6-311++G(2d,p) changes the number of these bond paths from 6 to 12. Since only a small change in the basis set cannot change the number of bonds, it is clear that interpreting the bond path as a bond is at least questionable.

The presented analysis was further enhanced by determining the Mayer Bond Order (MBO), which, contrary to the more popular, but somewhat outdated Wiberg Bond Index, may also have negative values. Indeed, *negative* MBO values were obtained for the Ng···C contacts, indicating their *anti*bonding nature.

Funding: This research received no external funding.

Conflicts of Interest: The author declares no conflict of interest.

Abbreviations

The following abbreviations are used in this manuscript:

Ng	noble gas (atom)
QTAIM	Quantum Theory of Atoms in Molecules (by R.F.W. Bader [1])
BP	bond path [1]
BCP	bond critical point [1]
WBI	Wiberg Bond Index [55]
MBO	Mayer Bond Order [56–59]

References

1. Bader, R.F.W. *Atoms in Molecules: A Quantum Theory*; Oxford University Press: New York, NY, USA, 1990.
2. Popelier, P.L.A. *Atoms in Molecules. An Introduction*; Longman: Singapore, 2000.
3. Matta, C.F.; Boyd, R.J. *The Quantum Theory of Atoms in Molecules*; Wiley-VCH: Weinheim, Germany, 2007.
4. Bader, R.F.W. A Bond Path: A Universal Indicator of Bonded Interactions. *J. Phys. Chem. A* **1998**, *102*, 7314–7323. [CrossRef]
5. Bader, R.F.W. A Quantum Theory of Molecular Structure and Its Appllcatlons. *Chem. Rev.* **1991**, *91*, 893–928. [CrossRef]
6. Cioslowski, J.; Mixon, S.T.; Edwards, W.D. Weak Bonds in the Topological Theory of Atoms in Molecules. *J. Am. Chem. Soc.* **1991**, *113*, 1083–1085. [CrossRef]
7. Cioslowski, J.; Mixon, S.T. Topological Properties of Electron Density in Search of Steric Interactions in Molecules: Electronic Structure Calculations on Ortho-Substituted Biphenyls. *J. Am. Chem. Soc.* **1992**, *114*, 4382–4387. [CrossRef]
8. Cioslowski, J.; Mixon, S.T. Universality among topological properties of electron density associated with the hydrogen–hydrogen nonbonding interactions. *Can. J. Chem.* **1992**, *70*, 443–449. [CrossRef]
9. Cioslowski, J.; Edgington, L.; Stefanov, B.B. Steric Overcrowding in Perhalogenated Cyclohexanes, Dodecahedranes, and [60]Fulleranes. *J. Am. Chem. Soc.* **1995**, *117*, 10381–10384. [CrossRef]
10. Haaland, A.; Shorokhov, D.J.; Tverdova, N.V. Topological Analysis of Electron Densities: Is the Presence of an Atomic Interaction Line in an Equilibrium Geometry a Sufficient Condition for the Existence of a Chemical Bond? *Chem. Eur. J.* **2004**, *10*, 4416–4421. [CrossRef]
11. Strenalyuk, T.; Haaland, A. Chemical Bonding in the Inclusion Complex of He in Adamantane (He@adam): The Origin of the Barrier to Dissociation. *Chem. Eur. J.* **2008**, *14*, 10223–10226. [CrossRef] [PubMed]
12. Cerpa, E.; Krapp, A.; Vela, A.; Merino, G. The Implications of Symmetry of the External Potential on Bond Paths. *Chem. Eur. J.* **2008**, *14*, 10232–10234. [CrossRef] [PubMed]
13. Cerpa, E.; Krapp, A.; Flores-Moreno, R.; Donald, K.J.; Merino, G. Influence of Endohedral Confinement on the Electronic Interaction between He atoms: A $He_2@C_{20}H_{20}$ Case Study. *Chem. Eur. J.* **2009**, *15*, 1985–1990. [CrossRef]
14. Tsirelson, V.G.; Zou, P.F.; Tang, T.-H.; Bader, R.F.W. Topological Definition of Crystal Structure: Determination of the Bonded Interactions in Solid Molecular Chlorine. *Acta Cryst.* **1995**, *A51*, 143–153. [CrossRef]
15. Bone, R.G.A.; Bader, R.F.W. Identifying and Analyzing Intermolecular Bonding Interactions in van der Waals Molecules. *J. Phys. Chem.* **1996**, *100*, 10892–10911. [CrossRef]
16. Abramov, Y.A. Secondary Interactions and Bond Critical Points in Ionic Crystals. *J. Phys. Chem. A* **1997**, *101*, 5725–5728 [CrossRef]
17. Vila, A.; Mosquera, R.A. On the perfluorination of alkyl ethers. An electron density study under the AIM approach. *J. Mol. Struct. (Theochem)* **2001**, *546*, 63–72. [CrossRef]
18. Luaña, V.; Costales, A.; Mori-Sánchez, P.; Pendás, A.M. Ions in Crystals: The Topology of the Electron Density in Ionic Materials. 4. The Danburite ($CaB_2Si_2O_8$) Case and the Occurrence of Oxide–Oxide Bond Paths in Crystals. *J. Phys. Chem. B* **2003**, *107*, 4912–4921. [CrossRef]
19. Matta, C.F.; Castillo, N.; Boyd R.J. Characterization of a Closed-Shell Fluorine–Fluorine Bonding Interaction in Aromatic Compounds on the Basis of the Electron Density. *J. Phys. Chem. A* **2005**, *109*, 3669–3681. [CrossRef] [PubMed]
20. Pakiari, A.H.; Eskandari, K. Closed shell oxygen–oxygen bonding interaction based on electron density analysis. *J. Mol. Struct. THEOCHEM* **2007**, *806*, 1–7. [CrossRef]
21. Palusiak, M.; Grabowski, S.J. Do intramolecular halogen bonds exist? Ab initio calculations and crystal structures' evidences. *Struct. Chem.* **2007**, *18*, 859–865. [CrossRef]
22. Jabłoński, M. Energetic and Geometrical Evidence of Nonbonding Character of Some Intramolecular Halogen···Oxygen and Other Y···Y Interactions. *J. Phys. Chem. A* **2012**, *116*, 3753–3764. [CrossRef] [PubMed]
23. Jabłoński, M.; Palusiak, M. The halogen···oxygen interaction in 3-halogenopropenal revisited—The *dimer model* vs. QTAIM indications. *Chem. Phys.* **2013**, *415*, 207–213. [CrossRef]
24. Dem'yanov, P.; Polestshuk, P. A Bond Path and an Attractive Ehrenfest Force Do Not Necessarily Indicate Bonding Interactions: Case Study on M_2X_2 (M = Li, Na, K; X = H, OH, F, Cl). *Chem. Eur. J.* **2012**, *18*, 4982–4993. [CrossRef]
25. Tognetti, V.; Joubert, L. On the physical role of exchange in the formation of an intramolecular bond path between two electronegative atoms. *J. Chem. Phys.* **2013**, *138*, 024102. [CrossRef]
26. Tognetti, V.; Joubert, L. On critical points and exchange-related properties of intramolecular bonds between two electronegative atoms. *Chem. Phys. Lett.* **2013**, *579*, 122–126. [CrossRef]
27. Jabłoński, M. Hydride-Triel Bonds. *J. Comput. Chem.* **2018**, *39*, 1177–1191. [CrossRef]
28. Jabłoński, M. Bond Paths Between Distant Atoms Do Not Necessarily Indicate Dominant Interactions. *J. Comput. Chem.* **2018**, *39*, 2183–2195. [CrossRef] [PubMed]
29. Jabłoński, M. On the Uselessness of Bond Paths Linking Distant Atoms and on the Violation of the Concept of Privileged Exchange Channels. *ChemistryOpen* **2019**, *8*, 497–507. [CrossRef] [PubMed]
30. Jabłoński, M. Counterintuitive bond paths: An intriguing case of the $C(NO_2)_3^-$ ion. *Chem. Phys. Lett.* **2020**, *759*, 137946. [CrossRef]
31. Matta, C.F.; Hernández-Trujillo, J.; Tang, T.-H.; Bader, R.F.W. Hydrogen-Hydrogen Bonding: A Stabilizing Interaction in Molecules and Crystals. *Chem. Eur. J.* **2003**, *9*, 1940–1951. [CrossRef] [PubMed]
32. Poater, J.; Solà, M.; Bickelhaupt, F.M. Hydrogen–Hydrogen Bonding in Planar Biphenyl, Predicted by Atoms-in-Molecules Theory, Does Not Exist. *Chem. Eur. J.* **2006**, *12*, 2889–2895. [CrossRef] [PubMed]

33. Poater, J.; Solà, M.; Bickelhaupt, F.M. A Model of the Chemical Bond Must Be Rooted in Quantum Mechanics, Provide Insight, and Possess Predictive Power. *Chem. Eur. J.* **2006**, *12*, 2902–2905. [CrossRef]
34. Dillen, J. Congested Molecules. Where is the Steric Repulsion? An Analysis of the Electron Density by the Method of Interacting Quantum Atoms. *Int. J. Quantum Chem.* **2013**, *113*, 2143–2153. [CrossRef]
35. Keyvani, Z.A.; Shahbazian, S.; Zahedi, M. To What Extent are "Atoms in Molecules" Structures of Hydrocarbons Reproducible from the Promolecule Electron Densities? *Chem. Eur. J.* **2016**, *22*, 5003–5009. [CrossRef] [PubMed]
36. Moran, D.; Woodcock, H.L.; Chen, Z.; Schaefer, H.F., III; Schleyer, P.V.R. On the Viability of Small Endohedral Hydrocarbon Cage Complexes: X@C_4H_4, X@C_8H_8, X@C_8H_{14}, X@$C_{10}H_{16}$, X@$C_{12}H_{12}$, and X@$C_{16}H_{16}$. *J. Am. Chem. Soc.* **2003**, *125*, 11442–11451. [CrossRef]
37. Darzynkiewicz, R.B.; Scuseria, G.E. Noble Gas Endohedral Complexes of C_{60} Buckminsterfullerene. *J. Phys. Chem. A* **1997**, *101*, 7141–7144. [CrossRef]
38. Schirch, P.F.T.; Boekelheide, V. [2.2.2.2.2](1,2,3,4,5)Cyclophane. *J. Am. Chem. Soc.* **1979** *101*, 3126–3127. [CrossRef]
39. Sekine, Y.; Boekelheide, V. A Study of the Synthesis and Properties of [2_6](1,2,3,4,5,6)Cyclophane (Superphane). *J. Am. Chem. Soc.* **1981**, *103*, 1777–1785. [CrossRef]
40. Gleiter, R.; Hopf, H. (Eds.) *Modern Cyclophane Chemistry*; Wiley-VCH: Weinheim, Germany, 2004.
41. Szabo, A.; Ostlund, N.S. *Modern Quantum Chemistry. Introduction to Advanced Electronic Structure Theory*; Dover Publications, Inc.: Mineola, NY, USA, 1982.
42. Becke, A.D. Density-functional exchange-energy approximation with correct asymptotic behavior. *Phys. Rev. A* **1988**, *38*, 3098–3100. [CrossRef]
43. Lee, C.; Yang, W.; Parr, R.G. Development of the Colle-Salvetti correlation-energy formula into a functional of the electron density. *Phys. Rev. B* **1988**, *37*, 785–789. [CrossRef]
44. Grimme, S.; Antony, J.; Ehrlich S.; Krieg, H. A consistent and accurate *ab initio* parameterization of density functional dispersion correction (DFT-D) for the 94 elements H-Pu. *J. Chem. Phys.* **2010**, *132*, 154104. [CrossRef]
45. Zhao, Y.; Truhlar, D.G. The M06 suite of density functionals for main group thermochemistry, thermochemical kinetics, noncovalent interactions, excited states, and transition elements: Two new functionals and systematic testing of four M06-class functionals and 12 other functionals. *Theor. Chem. Acc.* **2008**, *120*, 215–241.
46. Zhao, Y.; Truhlar, D.G. Density Functional for Spectroscopy: No Long-Range Self-Interaction Error, Good Performance for Rydberg and Charge-Transfer States, and Better Performance on Average than B3LYP for Ground States. *J. Phys. Chem. A* **2006**, *110*, 13126–13130. [CrossRef]
47. Chai, J.-D.; Head-Gordon, M. Long-range corrected hybrid density functionals with damped atom–atom dispersion corrections. *Phys. Chem. Chem. Phys.* **2008**, *10*, 6615–6620. [CrossRef]
48. Jensen, F. *Introduction to Computational Chemistry*; John Wiley & Sons Ltd.: Chichester, England, 2007.
49. Pritchard, B.P.; Altarawy, D.; Didier, B.; Gibson, T.D.; Windus, T.L. New Basis Set Exchange: An Open, Up-to-Date Resource for the Molecular Sciences Community. *J. Chem. Inf. Model.* **2019**, *59*, 4814–4820. [CrossRef] [PubMed]
50. Frisch, M.J.; Trucks, G.W.; Schlegel, H.B.; Scuseria, G.E.; Robb, M.A.; Cheeseman, J.R.; Scalmani, G.; Barone, V.; Petersson, G.A.; Nakatsuji, H.; et al. *Gaussian 16, Revision C.01*; Gaussian, Inc.: Wallingford, CT, USA, 2019.
51. Dennington, R.; Keith, T.; Millam, J. (Eds.) *GaussView, Version 6*; Semichem Inc.: Shawnee Mission, KS, USA, 2019.
52. Keith, T.A. *AIMAll (Version 15.05.18)*; TK Gristmill Software: Overland Park, KS, USA, 2015. Available online: aim.tkgristmill.com (accessed on 25 October 2021).
53. Jabłoński, M. A Critical Overview of Current Theoretical Methods of Estimating the Energy of Intramolecular Interactions. *Molecules* **2020**, *25*, 5512. [CrossRef] [PubMed]
54. Pauling, L. Atomic Radii and Interatomic Distances in Metals. *J. Am. Chem. Soc.* **1947**, *69*, 542–553. [CrossRef]
55. Wiberg, K.B. Application of the Pople-Santry-Segal CNDO Method to the Cyclopropylcarbinyl and Cyclobutyl Cation and to Bicyclobutane. *Tetrahedron* **1968**, *24*, 1083–1096. [CrossRef]
56. Mayer, I. Charge, bond order and valence in the AB initio SCF theory. *Chem. Phys. Lett.* **1983**, *97*, 270–274. [CrossRef]
57. Mayer, I. Bond order and valence: Relations to Mulliken's population analysis. *Int. J. Quantum Chem.* **1984**, *26*, 151–154. [CrossRef]
58. Mayer, I. Bond Order and Valence Indices: A Personal Account. *J. Comput. Chem.* **2007**, *28*, 204–221. [CrossRef] [PubMed]
59. Bridgeman, A.J.; Cavigliasso, G.; Ireland, L.R.; Rothery, J. The Mayer bond order as a tool in inorganic chemistry. *J. Chem. Soc. Dalton Trans.* **2001**, 2095–2108. [CrossRef]
60. Hohenberg, P.; Kohn, W. Inhomogeneous Electron Gas. *Phys. Rev.* **1964**, *136*, B864–B871. [CrossRef]
61. Parr, R.G.; Yang, W. *Density-Functional Theory of Atoms and Molecules*; Oxford University Press: New York, NY, USA, 1989.
62. Mardirossian, N.; Head-Gordon, M. Thirty years of density functional theory in computational chemistry: An overview and extensive assessment of 200 density functionals. *Mol. Phys.* **2017**, *115*, 2315–2372. [CrossRef]
63. Schreiner, P.R.; Chernish, L.V.; Gunchenko, P.A.; Tikhonchuk, E.Y.; Hausmann, H.; Serafin, M.; Schlecht, S.; Dahl, J.E.P.; Carlson, R.M.K.; Fokin, A.A. Overcoming lability of extremely long alkane carbon–carbon bonds through dispersion forces. *Nature* **2011**, *477*, 308–311. [CrossRef] [PubMed]
64. Fokin, A.A.; Chernish, L.V.; Gunchenko, P.A.; Tikhonchuk, E.Y.; Hausmann, H.; Serafin, M.; Dahl, J.E.P.; Carlson, R.M.K.; Schreiner, P.R. Stable Alkanes Containing Very Long Carbon–Carbon Bonds. *J. Am. Chem. Soc.* **2012**, *134*, 13641–13650. [CrossRef] [PubMed]

65. Ishigaki, Y.; Shimajiri, T.; Takeda, T.; Katoono, R.; Suzuki, T. Longest C–C Single Bond among Neutral Hydrocarbons with a Bond Length beyond 1.8 Å. *Chem* **2018**, *4*, 795–806. [CrossRef]
66. Brown, D.A.; Clegg, W.; Colquhoun, H.M.; Daniels, J.A.; Stephenson, I.R.; Wade, K. A pentuply-bridging carbonyl group: crystal and molecular structure of a salt of the 1-oxo-2-phenyl-1,2-dicarbadodecaborate(12) anion, $[LH]^+[O(Ph)C_2B_{10}H_{10}]^-$ (L = 1,8-*N*,*N*,*N*′,*N*′-tetramethylnaphthalenediamine). *J. Chem. Soc. Chem. Commun.* **1987**, 889–891. [CrossRef]
67. Llop, J.; Viñas, C.; Teixidor, F.; Victori, L.; Kivekäs, R.; Sillanpää, R. Redox Potential Modulation in Mixed Sandwich Pyrrolyl/Dicarbollide Complexes. *Inorg. Chem.* **2002**, *41*, 3347–3352. [CrossRef] [PubMed]
68. Li, J.; Pang, R.; Li, Z.; Lai, G.; Xiao, X.-Q.; Müller, T. Exceptionally Long C–C Single Bonds in Diamino-*o*-carborane as Induced by Negative Hyperconjugation. *Angew. Chem. Int. Ed.* **2019**, *58*, 1397–1401. [CrossRef] [PubMed]
69. Novoa, J.J.; Lafuente, P.; Del Sesto, R.E.; Miller, J.S. Exceptionally Long ($\geq$ 2.9 Å) C–C Bonds between $[TCNE]^-$ Ions: Two-Electron, Four-Center $\pi^\star$-$\pi^\star$ C–C Bonding in π-$[TCNE]_2^{2-}$. *Angew. Chem. Int. Ed.* **2001**, *40*, 2540–2545. [CrossRef]
70. Novoa, J.J.; Stephens, P.W.; Weerasekare, M.; Shum, W.W.; Miller, J.S. The Tetracyanopyrazinide Dimer Dianion, $[TCNE]_2^{2-}$. 2-Electron 8-Center Bonding. *J. Am. Chem. Soc.* **2009**, *131*, 9070–9075. [CrossRef]
71. Jabłoński, M. The first theoretical proof of the existence of a hydride-carbene bond. *Chem. Phys. Lett.* **2018**, *710*, 78–83. [CrossRef]
72. Møller, C.; Plesset, M.S. Note on an Approximation Treatment for Many-Electron Systems. *Phys. Rev.* **1934**, *46*, 618–622. [CrossRef]
73. Krapp, A.; Frenking, G. Is This a Chemical Bond? A Theoretical Study of $Ng_2@C_{60}$ (Ng = He, Ne, Ar, Kr, Xe). *Chem. Eur. J.* **2007**, *13*, 8256–8270. [CrossRef] [PubMed]
74. McNaught, A.D.; Wilkinson, A. *IUPAC Compedium of Chemical Terminology*; IUPAC: Research Triangle Park, NC, USA, 1997.
75. Belkacem, A.; Kanter, E.P.; Mitchell, R.E.; Wager, Z.; Zabransky, B.J. Measurement of the Ultrashort Bond Length in He_2^{++}. *Phys. Rev. Lett.* **1989**, *63*, 2555–2558. [CrossRef] [PubMed]
76. Ackermann, J.; Hogreve, H. On the metastability of the $^1\Sigma_g^+$ ground state of He_2^{2+} and Ne_2^{2+}: A case study of binding metamorphosis. *J. Phys. B At. Mol. Opt. Phys.* **1992**, *25*, 4069–4098. [CrossRef]
77. Kolbuszewski, M.; Gu, J.-P. Adiabatic and strictly diabatic potential curves of He_2^{2+}. *J. Chem. Phys.* **1995**, *103*, 7649–7650. [CrossRef]
78. Basch, H.; Aped, P.; Hoz, S. Valence bond energy curves for He_2^{2+}. *Chem. Phys. Lett.* **1996**, *255*, 336–340. [CrossRef]